

Supplementary Materials for Improved Estimation of the Open Boundary Conditions in Tidal Models Using Trigonometric Polynomials Fitting Scheme

1. Numerical simulation and comparison of K_1 constituent in Gulf of Thailand

The Gulf of Thailand are selected as the computation domain and the research object is K_1 tidal constituent. The simulation area covers $99^\circ E \sim 105^\circ E$, $1^\circ N \sim 14^\circ N$, with a horizontal resolution of $10' \times 10'$. The time step interval is set to be 359.018s, 1/240 of the period of K_1 tidal constituent. The bathymetry, the T/P-Jason altimeter tracks and the spatially varying BFCs of the Gulf of Thailand are shown in Figure S1.

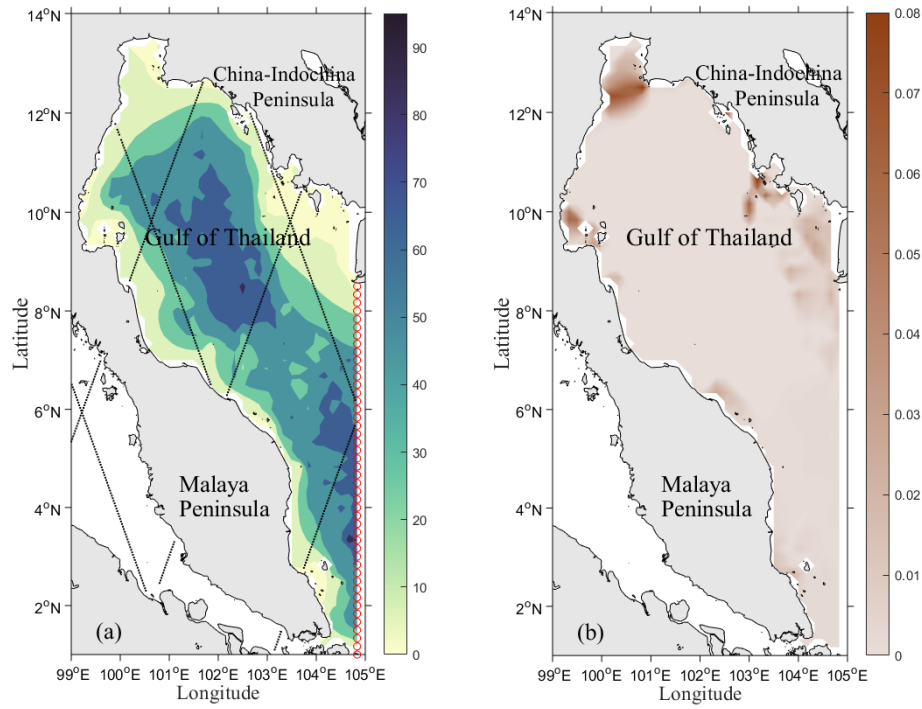


Figure S1. (a) The bathymetry (unit: m), open boundaries (red circles) and the T/P-Jason altimeter tracks. (b) The spatially varying BFCs of the Gulf of Thailand.

The OBCs of Gulf of Thailand are inverted by assimilating T/P-Jason altimeter data processed by X-TRACK to realize the numerical simulation of K_1 tidal constituent. Harmonic constants of the K_1 constituent along the T/P-Jason altimeter tracks are shown in Figure S2. The maximum number of iteration steps is set to 100, and the MTP in TPF scheme is set to 4. The estimated FCs and the descent process with iteration steps for the normalized cost function are shown in Figure S3.

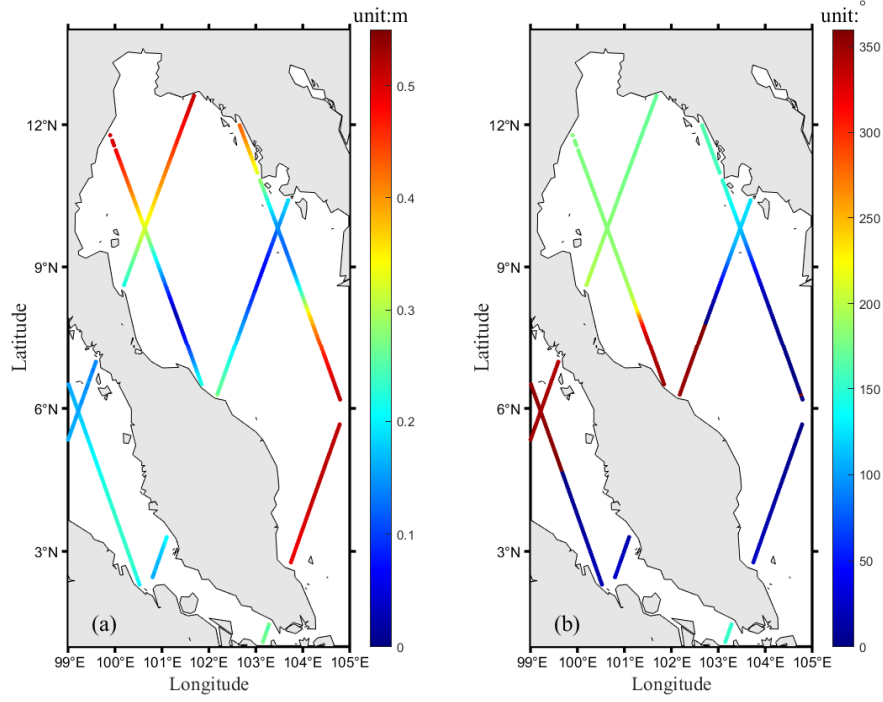


Figure S2. The amplitude (a) and phase (b) of K_1 constituent along T/P-Jason altimeter tracks in the Gulf of Thailand.

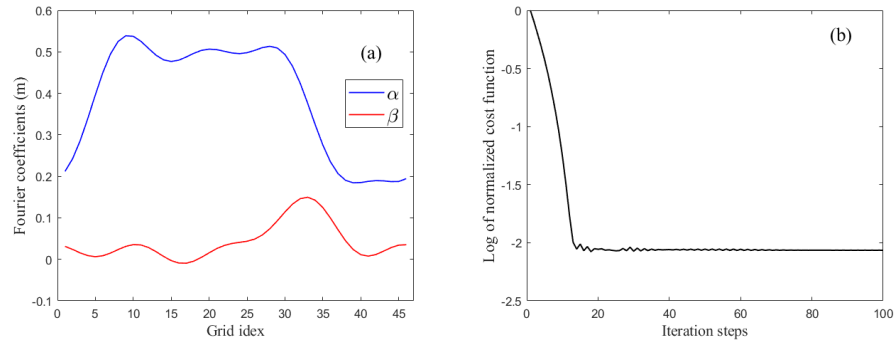


Figure S3. FCs (a) and the descent process with iteration steps for the normalized cost function (b) inverted by TPF scheme.

The FCs of harmonic constants from TPX09, FES2014 and EOT20 are calculated on the open boundary of the model domain (Figure S4). The forward model is driven with the FCs derived from model data, to obtain the simulations in the computation domain.

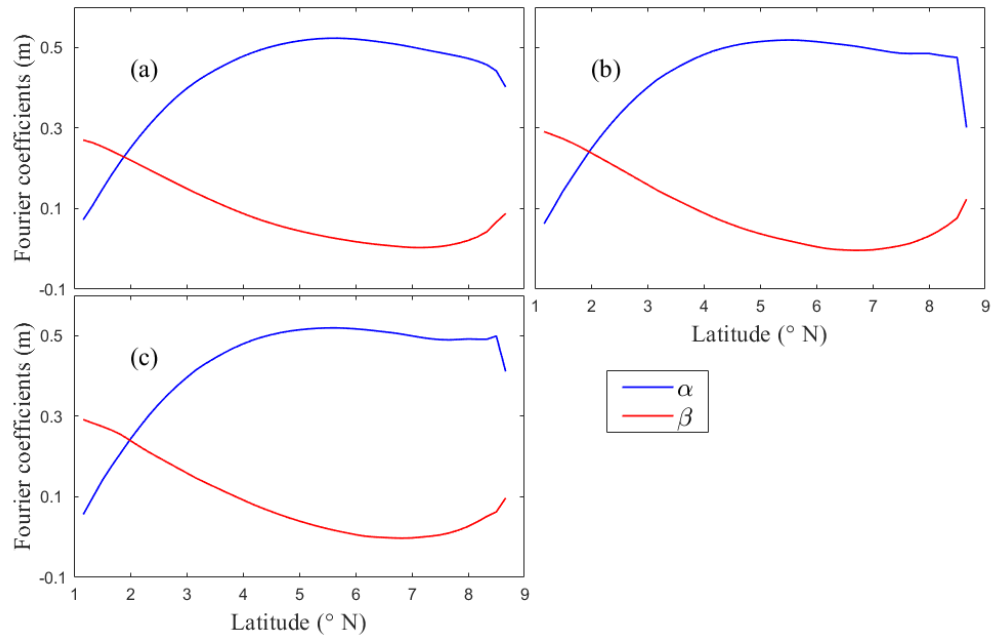


Figure S4. FCs of OBCs derived from model data TPXO9 (a), FES2014 (b), and EOT20 (c).

The differences between observations and simulations are calculate quantitatively. The MEA of harmonic constants and the RMS error between observations and simulations with different OBCs are shown in Table S1. The OBCs are estimated by data assimilation to reduce the error of simulations and observations.

Table S1. MAE and RMS errors between simulation and observations.

	MEA		RMS (cm)
	Amplitude (cm)	Phase (°)	
TPF	2.01	3.53	2.20
TPXO9	4.83	17.71	7.95
FES2014	4.66	18.70	8.22
EOT20	4.78	18.91	8.31

The Table S1 indicates that, simulations using OBCs obtained by TPF scheme are more advantageous than model data, with RMS error of 2.20 cm, the MAE of amplitude and phase are 2.01cm and 3.53° respectively. Simulation results using the OBCs derived from three model data have greater difference from the observations than those obtained through data assimilation.

Based on the OBCs estimated by assimilating T/P-Jason data using TPF scheme, the cotidal charts for the K_1 constituent in the Gulf of Thailand are drawn, as shown in Figure S5. The spatial distribution of the cotidal chart is in good agreement with the K_1 tidal constituent characteristics of the region. The amphidromic system appears counterclockwise, with amphidromic point near the west coast.

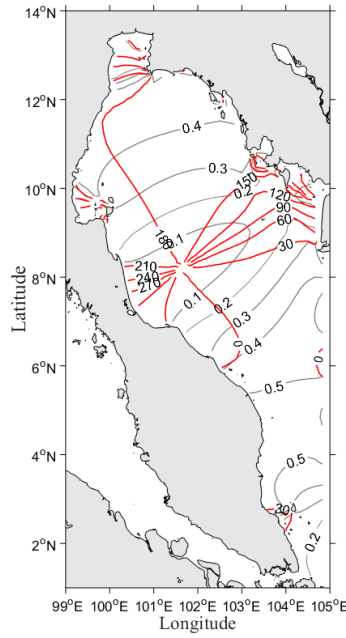


Figure S5. Cotidal chart for the K_1 constituent in the Gulf of Thailand obtained TPF scheme. Gray line denotes the co-amplitude line (m), red line denotes the co-phase line ($^{\circ}$).

2. Numerical simulation of S_2 , K_1 and O_1 tidal constituents in the BYS

The OBCs of BYS are inverted by assimilating T/P-Jason altimeter data processed by X-TRACK to realize the numerical simulation of the S_2 , K_1 and O_1 tidal constituents. The inversion process terminates when the number of iteration steps reaches 100, and the MTP is set as 3. The inverted FCs are shown in Figure S6.

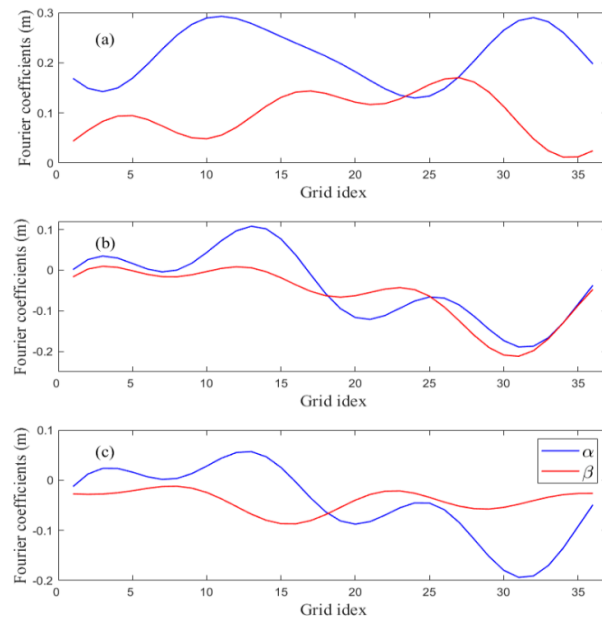


Figure S6. Inverted FCs of S_2 (a), K_1 (b) and O_1 (c) tidal constituents.

The differences between the simulated results and the observed ones are calculated respectively. The MAE of RMS error and harmonic constants are calculated (Table S2). The simulation results are also satisfactory, and the RMS errors of the three constituents are 1.31cm, 1.45cm and 1.23 cm respectively. According to the simulation results, the cotidal charts for the S_2 , K_1 and O_1 constituent in the BYS are drawn (Figure S7-S9).

Table S2. MAE and RMS errors between simulation and observations of different tidal constituents.

Tidal constituents	MAE		RMS (cm)
	Amplitude (cm)	Phase (°)	
S_2	0.96	2.29	1.31
K_1	1.14	2.73	1.45
O_1	0.88	3.29	1.23

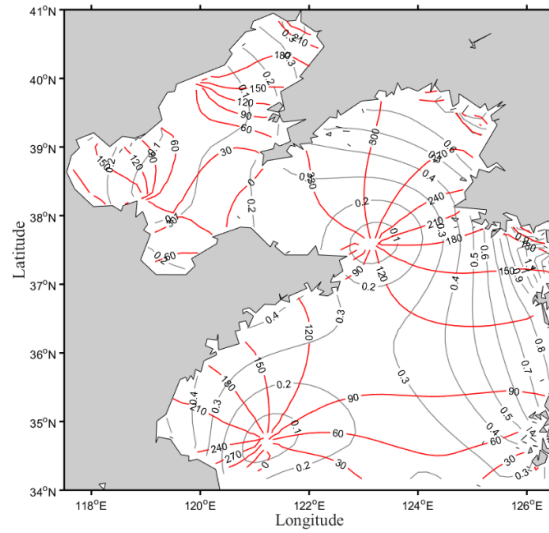


Figure S7. Cotidal chart for the S_2 constituent in the BYS obtained TPF scheme. Gray line denotes the co-amplitude line (m), red line denotes the co-phase line (°).

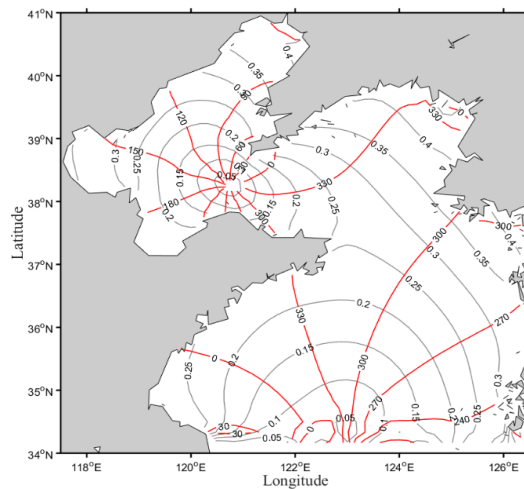


Figure S8. Similar to Figure S7, but for K_1 constituent.

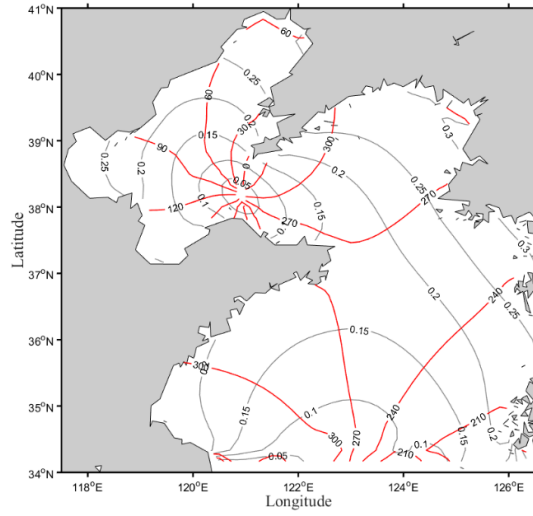


Figure S9. Similar to Figure S7, but for O_1 constituent.

The characteristics of S_2 tidal constituent are similar to that of M_2 tidal constituent. There are four amphidromic points in the BYS, including two in the Bohai Sea and two in the Yellow Sea. But the amplitude of the S_2 tidal constituent is much smaller than the M_2 tidal constituent. The characteristics of K_1 and O_1 constituents are similar, and there is an obvious amphidromic point in this area, located in the middle of the Bohai Strait. In addition, according to the trend of co-phase line, another amphidromic point can be found south of $34^\circ N$.